Z. Phys. B 94, 255–259 (1994)

ZEITSCHRIFT
FÜR PHYSIK B

a–b plane anisotropy of single-domain crystals of $Bi_2Sr_2CaCu_2O_8$

M.A. Quijada[1], **D.B. Tanner**[1], **R.J. Kelley**[2], **M. Onellion**[2]

[1] Department of Physics, University of Florida, Gainesville, FL 32611, USA (Fax: 1-904-392-3591; email: uftanner@nervm.nerdc.ufl.edu)
[2] Department of Physics, University of Wisconsin, Madison, WI 53706, USA

Received: 22 October 1993

Abstract. The polarized reflectance of the *a–b* plane of single-domain $Bi_2Sr_2CaCu_2O_8$ crystals is anisotropic above and below T_c. The normal-state infrared conductivity is higher for $\mathbf{E} \| a$ whereas the high-frequency conductivity is higher along *b*, particularly for transitions associated with the Bi−O layers. Below T_c there is a definite anisotropy to the far-infrared absorption, with a finite absorption for $\mathbf{E} \| b$ down to ~20 meV. This anisotropy of the *a–b* plane could be due either to anisotropy of the superconducting gap or to anisotropy of the midinfrared component to the conductivity.

PACS: 74.30.Gn; 74.70.Vy; 78.47.+p; 84.40.Cb

Superconductivity in the copper-oxide materials is associated with the quasi-two-dimensional CuO_2 planes. The anisotropy between the *c* axis and these *a-b* planes is large and well established. What is less well understood is the anisotropy within the *a-b* plane. There are two important questions about anisotropy: the anisotropy of the 2-*d* electronic structure in the normal state and the anisotropy of the superconducting order parameter.

The anisotropy of the superconducting order parameter is closely related both to the pairing mechanism and to the description of the normal state of these materials. Models like the marginal Fermi liquid picture lead to *s*-wave pairing [1, 2]. In the strong-coupling limit (or dirty limit) this *s*-wave gap is expected to be isotropic, even for strongly anisotropic materials [3]. Other models, mostly those which rely on antiferromagnetism for the pairing interaction, give a *d*-wave (essentially $d_{x^2-y^2}$) character to the order parameter. (See, for example, Refs. 4 and 5 and references therein). Recently, analyses of tunneling [6], photoemission [7], and penetration depth [8] have been advanced in support of such $d_{x^2-y^2}$ pairing. Other types of pairing, such as *p*-wave [9] and combinations of *s* and *d* wave states [10], have also been proposed.

Infrared spectroscopy is a direct probe of the anisotropic order parameter in unconventional superconductors [11]. However, in not every case does the anisotropy of the order parameter lead to an anisotropic *a-b*-plane optical conductivity. The conductivity for pure $d_{x^2-y^2}$ pairing is isotropic in the *a-b* plane (although the spectrum would of course be different from the case of *s*-wave pairing). In contrast, a *p*-wave component, a d_{xz} pairing, or a combination of *s*- and *d*-symmetries would give anisotropic *a-b*-plane optical conductivity.

Most previous infrared measurements of *a-b*-plane anisotropy have been for the 90-K transition-temperature $YBa_2Cu_3O_{7-\delta}$ material [12–16]. Much of the observed anisotropy of $YBa_2Cu_3O_{7-\delta}$ can be attributed to the quasi-one-dimensional CuO chains; their presence prevents determining whether the CuO_2 planes themselves have any intrinsic anisotropy. The Bi-based materials are better candidates for investigating the issue of *a-b*-plane anisotropy because there are no chains in these compounds. In the so-called 2212 phase, $Bi_2Sr_2CaCu_2O_8$ ($T_c = 85$ K), the CuO_2 planes are separated by Bi-O double layers, which are believed to act as a charge reservoir. There is an orthorhombic distortion of the nearly tetragonal *ab*-plane on account of a long-range superlattice modulation of the Bi-O layers [17].

Several authors [18–27] have reported optical studies of $Bi_2Sr_2CaCu_2O_8$. Only a few measurements have addressed the polarization dependence within the *a-b* plane. Ellipsometric measurements [19] in the near-infrared-ultraviolet find a strong anisotropy, with a transition at 3.8 eV stronger and sharper for light polarized along the modulation direction. *a-b*-plane anisotropy has also been observed in the far-infrared transmittance of free standing single crystals [24]. In this paper we present a detailed study of the *a-b*-plane anisotropy in the optical reflectance for untwinned samples of $Bi_2Sr_2CaCu_2O_8$ in a wide frequency range (Far-IR-UV) and for temperatures above and below the superconducting transition temperature.

The single crystals used in this study were grown as described by Han et al. [28]. Typical crystals are thin rectangular platelets with a surface area of a few milli-

meters square in the *a-b* plane. Four-probe resistance gives a zero resistance at typically 83 K with a transition width of ~4 K. The principal axes were identified from the extinction points when rotating the sample in a microscope with crossed polarizers; they correlate with the *a* and *b* directions as observed with LEED, where *b* is the superlattice direction. Note that in the $Bi_2Sr_2CaCu_2O_8$ structure the *a* and *b* axes are along the Bi-O bonds, nearly 45° from the Cu-O bonds.

The polarized reflectance was measured at near-normal incidence. In the high energy (1000–35 000 cm^{-1}) range we used a grating spectrometer (Perkin-Elmer 16U) while the far- and mid-infrared (80–4000 cm^{-1}) regions were measured with a Fourier spectrometer (Bruker IFS 113v). For the latter frequencies, the temperature of the sample was varied between 300 and 20 K using a flow cryostat. In order to determine the absolute value of the reflectance in the far-IR, we Al coated the samples and measured the reflectance of the coated sample. This procedure gives a reference standard with an area equal to that of the $Bi_2Sr_2CaCu_2O_8$ crystal. The far-IR spectrum of the uncoated sample was then divided by the spectrum of the coated sample and corrected for the known reflectance of Al. The accuracy in absolute reflectance, estimated from reproducibility of three different samples, is ±1%. However, the accuracy of the anisotropy of the reflectance is better than ±0.25%.

Figure 1 shows the room temperature reflectance on a wide frequency scale for polarization perpendicular and parallel to the superlattice directions in $Bi_2Sr_2CaCu_2O_8$ (labeled as *a* and *b* axes respectively). First, we notice that at low frequencies the *a*-axis reflectance is higher than the *b*-axis reflectance by 1–2%. As the frequency increases, the reflectance falls off in a quasilinear fashion. The plasmon minimum for the *b*-axis polarization occurs at a slightly lower frequency than in the *a*-axis direction. The splitting is estimated to be around 500 cm^{-1}. The in-plane anisotropy of $Bi_2Sr_2CaCu_2O_8$ is less pronounced than in untwinned $YBa_2Cu_3O_{7-\delta}$, where the splitting is

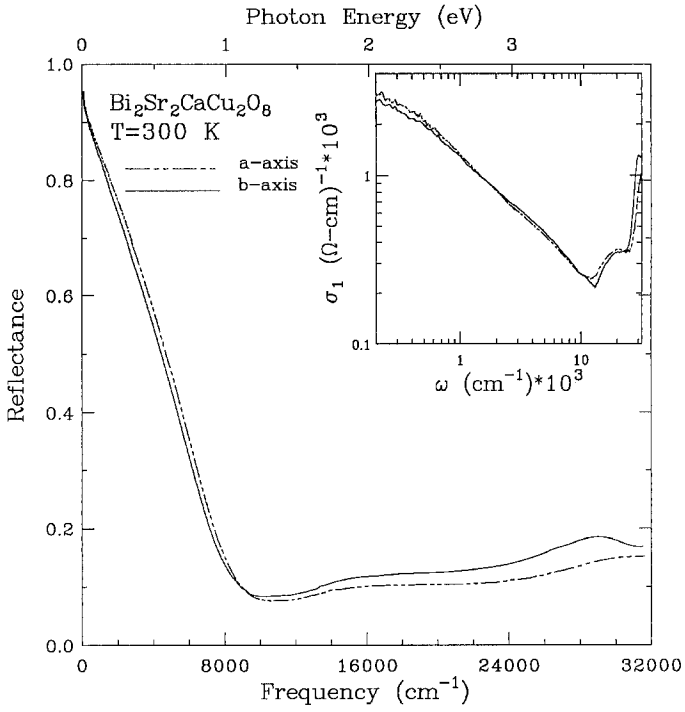

Fig. 1. The 300 K reflectance over a wide frequency range for light polarized along the *a* and *b* axes in $Bi_2Sr_2CaCu_2O_8$. Inset: conductivity obtained from Kramers-Kronig analysis of the reflectance. (Notice the logarithmic axes)

[12] ~5500 cm^{-1}. The fact that we are able to observe anisotropy in $Bi_2Sr_2CaCu_2O_8$, which does not have chains, indicates the electronic structure of the quasi-2-dimensional CuO_2 and/or Bi-O planes is anisotropic. Because the Cu-O bond lengths differ more in $YBa_2Cu_3O_{7-\delta}$ than in $Bi_2Sr_2CaCu_2O_8$, we would expect that the CuO_2-layer anisotropy is larger in the former compound, although it cannot be separated from the anisotropy introduced by the chains.

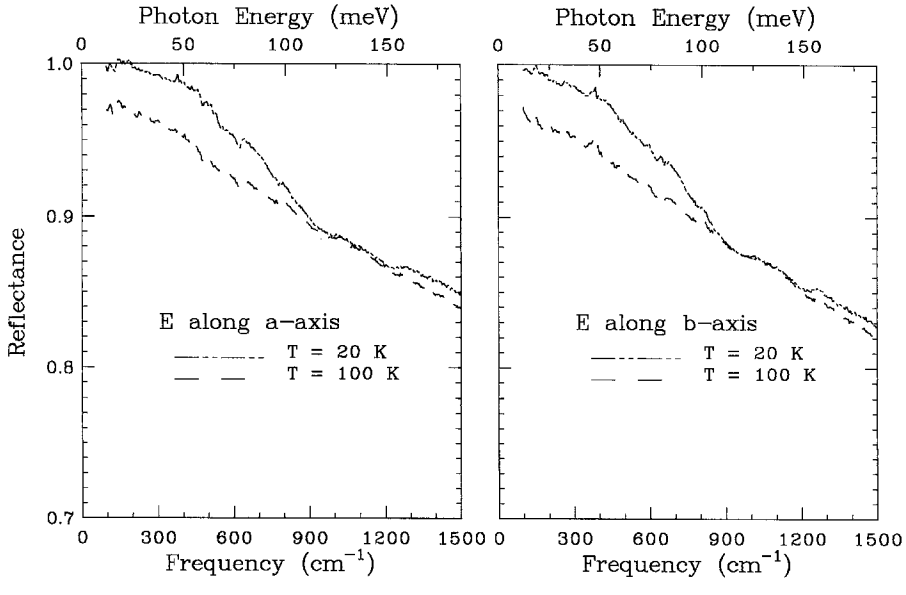

Fig. 2. Left panel: Far- and midinfrared *a*-axis reflectance of $Bi_2Sr_2CaCu_2O_8$ at 20 and 100 K. Right panel: *b*-axis reflectance at the same temperatures

We find the reflectance is substantially higher for $\mathbf{E}\|b$ for frequencies above the plasmon minimum. In addition two interband peaks are evident in this region. The first interband peak at ~ 2.3 eV is present in both polarizations whereas the second peak centered around 3.8 eV is more pronounced for the polarization along b and is almost absent along the a direction. The 2.3 eV peak is interpreted as the charge transfer band of the CuO_2 planes, whereas the 3.8 eV one is most likely associated with transitions occurring in the Bi-O layers and not in the CuO_2 planes [23]. Our measurements confirm earlier ellipsometric measurements done by Kelly et al. [20]. Moreover the stronger high-frequency bands along b provide a larger background polarizability to screen the low-frequency carriers, accounting for the lower plasmon frequency for the b-axis polarization.

We calculated the optical constants using Kramers-Kronig analysis of the reflectance. The results for the 300 K optical conductivity, $\sigma_1(\omega)$, are shown in the inset of Fig. 1. The electronic bands that were seen in the reflectance are all evident here. The far-infrared conductivity is close to the dc value; with increasing frequency $\sigma_1(\omega)$ falls quasi-linearly, as is typical of the oxide superconductors [29, 30].

The low temperature reflectance is shown for both polarizations in Fig. 2. The far infrared reflectance is higher for $\mathbf{E}\|a$ at all temperatures. Romero et al. [24] found that the in-plane transmittance of free standing single crystals of $Bi_2Sr_2CaCu_2O_8$ is higher for light polarized along the a-axis, implying more absorption for the b-polarization. Our reflectance results agree with this earlier report. In the superconducting state, a difference of 1–2% remains in the far-infrared reflectance ($\mathscr{R}_a > \mathscr{R}_b$). Although our accuracy in absolute reflectance is only $\pm 1\%$, implying that we cannot determine whether the a-axis reflectance is unity or not below $200\,\mathrm{cm}^{-1}$, our accuracy in measuring anisotropy is estimated at $\pm 0.25\%$, so that we can say with certainty that the b-axis reflectance is *less than* 100% down to $\sim 150\,\mathrm{cm}^{-1}$ (~ 20 meV).

The temperature evolution of the conductivity is shown in Fig. 3. In the normal state, we observe a sharpening and an increase of the low frequency conductivity at low temperatures, in accord with the increasing dc conductivity. Much of the finite-frequency oscillator strength is removed by the superconducting transition. There is a weak minimum in the superconducting state $\sigma_1(\omega)$ around $\omega \sim 450\,\mathrm{cm}^{-1}$. In some studies, this structure in the conductivity of the CuO_2 plane has been interpreted as the superconducting energy gap [13]. The fact that we observe the minimum for the polarization along b, where the reflectance is less than 100%, would disagree with the conventional notion of the gap as the threshold for quasiparticle excitations. We should point out that photoemission experiment done on samples from the same batch as the ones used in this study have shown convincing evidence for the opening of a gap in the density of states at the Fermi level [31]. The gap parameter obtained from the analysis of the photoemission places 2Δ close to $400\,\mathrm{cm}^{-1}$ (50 meV). Although this energy is near the minimum observed in the conductivity data, the finite absorption (in both polarizations but particularly in b) is inconsistent with a superconducting energy gap in the BCS sense. Because this structure has been observed in many cuprate superconductors, it has been attributed to strong bound carrier-phonon coupling [32].

Figure 4 shows for two crystals the anisotropy in the absorptivity ($A_b - A_a \equiv \mathscr{R}_a - \mathscr{R}_b$) in the superconducting state. This result illustrates the definite absorption for $\mathbf{E}\|b$ down to $\omega \sim 150\,\mathrm{cm}^{-1}$. This increased absorptivity ($\sim 1\%$) leads to the larger superconducting state conductivity of Fig. 3.

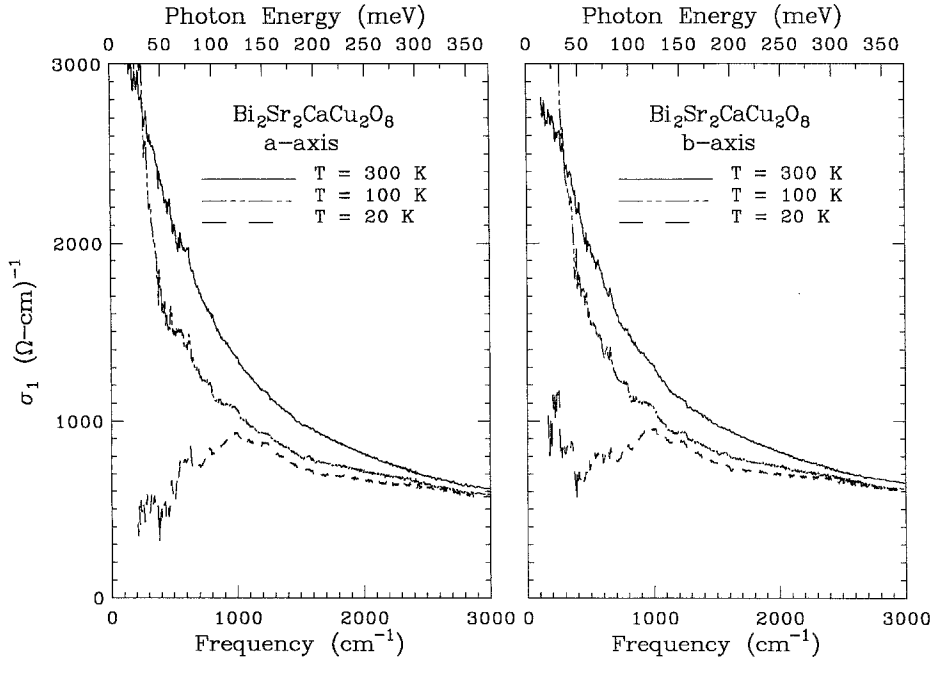

Fig. 3. Left panel: Temperature dependence of the a-axis conductivity of $Bi_2Sr_2CaCu_2O_8$ in the infrared. Right panel: Results for the b axis

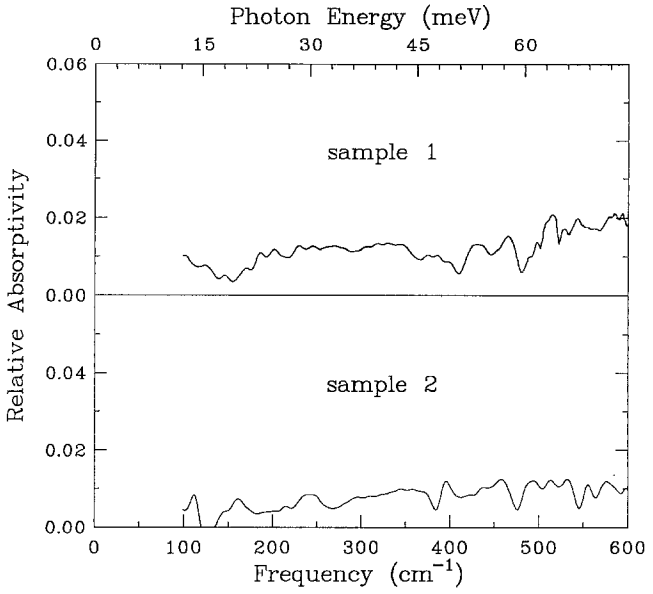

Fig. 4. The anisotropy in absorptivity ($A_b - A_a$) at 20 K for two different $Bi_2Sr_2CaCu_2O_8$ crystals

It is difficult to quantify whether this observed superconducting-state anisotropy is "large" or "small", either on an absolute scale or in relation to the anisotropy of the normal state. The anisotropy in reflectance is relatively modest, being of order 1% both above and below T_c. However, because the $\mathbf{E} \| a$ absorptivity is nearly zero below T_c whereas it is finite above T_c, the anisotropy in absorptivity is much larger in the superconducting state than in the normal state. Perhaps the most quantitative statement that we can make is that $\sigma_{1a}(\omega)$ and $\sigma_{1b}(\omega)$ differ at the lowest frequency ($\sim 150\,\mathrm{cm}^{-1}$ or ~ 20 meV) by about a factor of two below T_c whereas they differ by only 10% at 100 K. (See Fig. 3.)

There are two interpretations that we can advance for this low-frequency anisotropy below T_c, closely related to the issue of the non-Drude behavior of the midinfrared conductivity. In one view, there is a single component to the conductivity, with the observed normal-state spectrum attributed to a frequency dependent relaxation rate for the charge carriers [1, 13, 16]. The superconducting-state conductivity is then due to excitations across the superconducting gap, a gap which is anisotropic. If this interpretation is adopted, our data are incompatible with *s*-wave pairing or with a pure $d_{x^2-y^2}$ gap; they would be compatible with a *p*-wave gap, with certain combinations of *s* and *d* pairing [10], or with some *d*-wave order parameters (such as d_{xz}). Recent photoemission measurements by two of us [33] suggest a d_{xz} or p_x symmetry for the superconducting condensate.

The second interpretation regards the optical conductivity as being composed of two distinct components: a free-carrier component responsible for the low-frequency optical and *dc* normal-state conductivity coexisting with a second component which governs the midinfrared optical properties. Below T_c most of the free carriers condense to form the superfluid (giving a delta-function contribution to the conductivity) and the remaining finite-frequency conductivity is due to the midinfrared carriers. Two-component (or Drude plus midinfrared) analyses have been carried out many times previously [29, 34]; our results are compatible with these earlier studies: the Drude and the midinfrared components have nearly equal oscillator strengths; the Drude relaxation rate is linear in temperature above T_c, in accord with the *dc* conductivity; and the midinfrared component has very little temperature dependence. We can obtain reasonably good (although not unique) fits with an essentially isotropic oscillator strength for both the free carrier and midinfrared components [35]. The anisotropy is then due to two factors. Above T_c, the free carrier damping is 25% stronger along *b*. [$1/\tau(100\,\mathrm{K}) = 150\,\mathrm{cm}^{-1}$ for the *b* axis and $120\,\mathrm{cm}^{-1}$ for the *a* axis.] Above *and* below T_c there is a larger low frequency tail from the midinfrared conductivity along the *b* axis than along the *a* axis. This anisotropy is compatible with the observed orthorhombic unit cell, with recent photoemission results [36], and points to a definite anisotropy of the electronic structure within the *a*-*b* plane.

In sum, there are two ways that we can understand the observed *a*-*b*-plane anisotropy in $Bi_2Sr_2CaCu_2O_8$. One implies an unconventional nature to the superconducting pairing while the other suggests an unusual two-component nature of the low energy electronic structure. While we can not make a choice between these two pictures, our data do appear to rule out the commonly used model of an *s*-wave gap in a one-component picture of the oxide superconductors as well as a one-component picture with a $d_{x^2-y^2}$ gap.

We thank Peter Hirschfeld, Robert Joynt, and Chandra Varma for useful conversations. This research is supported by National Science Foundation grants DMR-9101676 (Florida) and DMR-8911332 (Wisconsin).

References

1. Varma, C.M., Littlewood, P.B., Schmitt-Rink, S., Abrahams, E., Ruckenstein, A.: Phys. Rev. Lett. **63**, 1996 (1989); ibid. **64**, 497 (1990) (E)
2. Littlewood, P.B., Varma, C.M.: Phys. Rev. B**46**, 405 (1992)
3. Combescot, R.: Phys. Rev. Lett. **67**, 148 (1991)
4. Schrieffer, J.R., Wen, X.G., Zhang, S.C.: Phys. Rev. B**39**, 11663 (1989)
5. Monthoux, P., Balatsky, A.V., Pines, D.: Phys. Rev. B**46**, 14803 (1992); Monthoux, P., Pines, D.: Phys. Rev. B**47**, 6069 (1993)
6. Coffey, D., Coffey, L.: Phys. Rev. Lett. **70**, 1529 (1993)
7. Shen, Z.-X., Dessau, D.S., Wells, B.O., King, D.M., Spicer, W.E., Arko, A.J., Marshall, D., Lombardo, L.W., Kapitulnik, A., Dickinson, P., Doniach, S., DiCarlo, J., Loeser, A.G., Park, C.H.: Phys. Rev. Lett. **70**, 1553 (1993)
8. Hardy, W.N., Bonn, D.A., Morgan, D.C., Ruixing Liang, Kuan Zhang: Phys. Rev. Lett. **70**, 3999 (1993)
9. Monien, H., Zawadowski, A.: Phys. Rev. Lett. **63**, 911 (1989)
10. Li, Q.P., Koltenbah, B.E.C., Joynt, R.: Phys. Rev. B**48**, 437 (1993)
11. Hirschfeld, P.J., Puttika, W.O., Wölfle, P.: Phys. Rev. Lett. **69**, 1447 (1992)
12. Koch, B., Geserich, H.P., Wolf, T.: Solid State Commun. **71**, 495 (1989)
13. Schlesinger, Z., Collins, R.T., Holtzberg, F., Feild, C., Blanton, S.H., Welp, U., Crabtree, G.W., Fang, Y., Liu, J.Z.: Phys. Rev. Lett. **65**, 801 (1990)

14. Pham, T., Drew, H.D., Moseley, S.H., Liu, J.Z.: Phys. Rev. B**44**, 5377 (1991)
15. Rotter, L.D., Schlesinger, Z., Collins, R.T., Holtzberg, F., Field, C., Welp, U., Crabtree, G.W., Liu, J.Z., Fang, Y., Vandervoort, G., Fleshler, S.: Phys. Rev. Lett. **67**, 2741 (1991)
16. Cooper, S.L., Kotz, A.L., Karlow, M.A., Klein, M.V., Lee, W.C., Giapintzakis, J., Ginsberg, D.M.: Phys. Rev. B**45**, 2549 (1992)
17. Shaw, T.M., Shivashankar, S.A., La Placa, S.J., Cuomo, J.J., McGuire, T.R., Roy, R.A., Kelleher, K.H., Yee, D.S.: Phys. Rev. B**37**, 9856 (1988)
18. Reedyk, M., Bonn, D.A., Garrett, J.D., Greedan, J.E., Stager, C.V., Timusk, T., Kamarás, K., Tanner, D.B.: Phys. Rev. B**38**, 11981 (1988)
19. Kelly, M.K., Barboux, P., Tarascon, J.-M., Aspnes, D.E., Morris, P.A., Bonner, W.A.: Physica C**162–164**, 1123 (1989)
20. Kelly, M.K., Barboux, P., Tarascon, J.-M., Aspnes, D.A.: Phys. Rev. B**40**, 6797 (1989)
21. Humlicek, J., Schmidt, E., Bocanek, L., Garriga, M., Cardona, M.: Solid State Commun. **73**, 127 (1990)
22. Terasaki, I., Tajima, S., Eisaki, H., Takagi, H., Uchinokura, K., Uchida, S.: Phys. Rev. B**41**, 865 (1990)
23. Yun-Yu Wang, Ritter, A.L.: Phys. Rev. B**43**, 1241 (1991)
24. Romero, D.B., Carr, G.L., Tanner, D.B., Forro, L., Mandrus, D., Mihály, L., Williams, G.P.: Phys. Rev. B**44**, 2818 (1991)
25. Romero, D.B., Porter, C.D., Tanner, D.B., Forro, L., Mandrus, D., Mihaly, L., Carr, G.L., Williams, G.P.: Phys. Rev. Lett. **68**, 1590 (1992)
26. Zibold, A., Dürrler, M., Gaymann, A., Geserich, H.P., Nücker, N., Burlakov, V.M., Müller, P.: Physica C**193**, 171 (1992)
27. Kamarás, K., Herr, S.L., Gao, F., Andraka, B., Stewart, G.R., Tanner, D.B., Etemad, S., Remschnig, K., Tarascon, J.-M.: In: Proceedings of the International Winterschool on Electronic Properties of High-Temperature Superconductors (1992)
28. Han, P.D., Payne, D.A.: J. Crystal Growth **104**, 201 (1990)
29. Tanner, D.B., Timusk, T.: In: Physical Properties of High Temperature Superconductors III. Ginsberg, D.M. (ed.), p. 363. Singapore: World Scientific 1992
30. The actual slope in the 400–8000 cm^{-1} region is $\omega^{-0.56\pm0.02}$
31. Hwu, Y., Lozzi, L., Marsi, M., La Rosa, S., Winokur, M., Davis, P., Onellion, M., Berger, H., Gozzo, F., Lévy, F., Margaritondo, G.: Phys. Rev. Lett. **67**, 2573 (1991)
32. Timusk, T., Porter, C.D., Tanner, D.B.: Phys. Rev. Lett. **66**, 663 (1991)
33. Kelley, R.J., Jian Ma, Margaritondo, G., Onellion, M.: Phys. Rev. Lett. **71**, 4051 (1993)
34. Timusk, T., Tanner, D.B., in Physical Properties of High Temperature Superconductors I. Ginsberg, D.M. (ed.), p. 339. Singapore: World Scientific 1989
35. The best fits to Drude-Lorentz models give free-carrier plasma frequencies of $\omega_{pD}^{a}=9000\pm300\ cm^{-1}$ and $\omega_{pD}^{b}=8700\pm400\ cm^{-1}$ ($\sim$1.1 eV in both cases). The broad (2000 cm^{-1} width) mid-infrared band is at $\sim$700 cm^{-1} in both polarizations and has plasma frequencies of $\omega_{p\mathrm{mir}}^{a}=10\,000\pm500\ cm^{-1}$ and $\omega_{p\mathrm{mir}}^{b}=10\,100\pm500\ cm^{-1}$, ($\sim$1.2 eV) respectively
36. Kelley, R.J., Jian Ma, Onellion, M., Marsi, M., Alméras, P., Berger, H., Margaritondo, G.: Phys. Rev. B**48**, 3534 (1993)